Early entombment within silica minimizes the molecular degradation of microorganisms during advanced diagenesis

Julien Alleon, Sylvain Bernard, Corentin Le Guillou, Damien Daval, Feriel Skouri-Panet, Sylvain Pont, Ludovic Delbes, François Robert

Chemical Geology 437 (2016) 98–108

Contents lists available at ScienceDirect

Chemical Geology

journal homepage: www.elsevier.com/locate/chemgeo

Early entombment within silica minimizes the molecular degradation of microorganisms during advanced diagenesis

Julien Alleon [a], Sylvain Bernard [a], Corentin Le Guillou [a,b], Damien Daval [c], Feriel Skouri-Panet [a], Sylvain Pont [a], Ludovic Delbes [a], François Robert [a]

[a] IMPMC, CNRS UMR 7590, MNHN, UPMC, 61 rue Buffon, 75005 Paris, France
[b] UMET, CNRS UMR 8207, Univ Lille 1, 59655 Villeneuve d'Ascq, France
[c] LHyGeS, CNRS UMR 7517, Université de Strasbourg/EOST, 1 Rue Blessig, 67084 Strasbourg, France

ARTICLE INFO

Article history:
Received 25 March 2016
Received in revised form 28 May 2016
Accepted 30 May 2016
Available online 01 June 2016

Keywords:
Experimental silicification
Experimental fossilization
Organic microfossils
Molecular biosignatures
XANES spectroscopy

ABSTRACT

Most ancient organic microfossils delicately preserved in 3D have been found in cherts. Although entombment within silica has been shown to promote morphological preservation, the impact of early silicification on the molecular evolution of fossilized microorganisms during burial remains poorly constrained. Here, we report results of advanced fossilization experiments performed under pressure (250 bars) and temperature (250 °C) conditions typical of sub-greenschist facies metamorphism for different durations up to 100 days on microorganisms experimentally entombed (or not) within a silica gel. The experimental residues have been characterized using XRD and XANES spectroscopy. The present study demonstrates that entombment within silica limits the degradation of microorganism molecular signatures, likely through specific chemical interactions, despite the progressive conversion of silica into quartz during the experiments. Extrapolation of the present results suggests that such protection may persist during geological timescales. The present experimental study provides molecular evidence that, in addition to morphologies, cherts may support the chemical preservation of remains of ancient life. The present results thus constitute a step forward towards the reconstruction of the original chemistry of putative fossilized microorganisms.

1. Introduction

Ancient organic microfossils provide a great deal of information about the evolution of cellular life on Earth. Yet, in addition to hindering their identification, the inevitable degradation of the organic molecules comprising these microorganisms over the course of geologic time likely muddles the reconstruction of their original chemistry (e.g. Bernard and Papineau, 2014; Briggs and Summons, 2014). As a result, the search for the earliest fossil evidence of life on Earth has been and is still fraught with controversies (e.g. Schopf et al., 2002; Brasier et al., 2002; Schopf and Kudryavtsev, 2012; Brasier et al., 2015; Wacey et al., 2015).

Remarkably, most of the oldest (putative) organic microfossils delicately preserved in 3D reported so far have been found in cherts (*i.e.* silica-rich rocks), (e.g. Walsh and Lowe, 1985; Ueno et al., 2001, 2006; Westall et al., 2001, 2006, 2011, 2015; Tice and Lowe, 2004, 2006; Sugitani et al., 2007, 2010, 2013, 2015a, 2015b; Glikson et al., 2008; Javaux et al., 2010; Wacey et al., 2011a, 2011b, 2012; Lepot et al., 2013). Cherts are thus now recognized as windows of exceptional morphological preservation of organic microfossils (i.e. "Bitter Springs-type preservation", sensu Butterfield, 2003; Xiao and Schiffbauer, 2009). Despite this recognition and recent analytical progress, studies addressing the molecular signatures of (putative) organic microfossils morphologically preserved in ancient cherts remain rare (e.g., De Gregorio and Sharp, 2006; Igisu et al., 2009; De Gregorio et al., 2009, 2011; Alleon et al., 2016). Intriguingly, although these (putative) microfossils have experienced diagenetic temperatures similar to overmature clay-rich gas shales, *i.e.* prehnite-pumpellyite to greenschist facies metamorphism, their molecular signatures are significantly less degraded than those of overmature kerogens (Bernard et al., 2010b, 2012a, 2012b).

A priori, silicification might be invoked as the explanation for the limited molecular degradation experienced by these microfossils during advanced (thermal) diagenesis. The critical role of authigenic mineralization (e.g.., pyritization, calcification, phosphatization, chloritization, glauconitization) in the morphological survivability of organic fossils through geological times has indeed been recognized and highlighted by many authors (e.g., Orr et al., 1998; Briggs, 2003; Briggs and Wilby, 1996; Bernard et al., 2010a; Anderson et al., 2011; Galvez et al., 2012; Kremer et al., 2012; Broce et al., 2014; Schiffbauer et al., 2014; Wacey et al., 2014; Muscente et al., 2015). Consistently, a number of experimental studies have highlighted the importance of the close association with minerals (such as sulfides, carbonates, phosphates, hydroxides, clays) for the morphological (e.g., Briggs and Kear, 1993; Briggs et al., 1993; Grimes et al., 2001; Martin et al., 2003; Wilson and Butterfield,

http://dx.doi.org/10.1016/j.chemgeo.2016.05.034
0009-2541/

2014; Iniesto et al., 2015) and chemical (e.g., Li et al., 2013, 2014; Picard et al., 2015a, 2015b) preservation/degradation of soft tissues during fossilization processes.

Silicification processes have received even more attention: silicified microbial morphologies have been studied *in situ* by many authors in modern silicifying hydrothermal systems (Walter et al., 1972; Schultze-Lam et al., 1995; Cady and Farmer, 1996; Konhauser and Ferris, 1996; Jones et al., 1998, 2001, 2003, 2004; McKenzie et al., 2001; Konhauser et al., 2001, 2003, 2004; Handley et al., 2005, 2008; Campbell et al., 2015). In parallel, a number of authors have experimentally investigated the processes of silica polymerization and precipitation in the presence of microorganisms (e.g. Fortin and Ferris, 1998; Hinman, 1990; Fein et al., 2002; Yee et al., 2003; Benning et al., 2004a, 2004b). Further, the impact of early silicification on the morphologies of microorganisms has been extensively studied through laboratory experiments conducted under various conditions, from room temperature to pressure and temperature conditions typical of diagenesis (e.g. Oehler and Schopf, 1971; Oehler, 1976a; Walters et al., 1977; Francis et al., 1978a, 1978b; Birnbaum et al., 1989; Westall et al., 1995; Phoenix et al., 2000; Toporski et al., 2002; Lalonde et al., 2005; Orange et al., 2009, 2011a, 2011b, 2012, 2013a, 2013b, 2014).

Altogether, these studies have shown that the precipitation of amorphous silica is mainly controlled by the dehydroxylation of the active hydroxyl groups present at the surface of silica (silanols) and that the rate of amorphous silica polymerization and precipitation is independent of the presence of biomass, *i.e.* that the microbial role in silicification is predominantly incidental. During silicification, microorganisms likely act as templates for the binding and nucleation of silica, even though they have only little affinity for monomeric silica. Long exposure to silicifying media eventually leads to the complete impregnation of microorganisms by silica, with cell walls and intracellular granules progressively becoming the only recognizable features. Besides the pioneering study of Oehler (1976a), which investigated the geochemical evolution of algal soluble organics (lipids and pigments) during thermal diagenesis, and the recent study of Orange et al. (2012), which documented the changes in composition of archeal soluble organics (amino acids, polysaccharides and lipids) during silicification, the above-mentioned experimental studies have all only focused on morphologies. Although these studies have highlighted the high potential of silica matrices for the morphological preservation of microfossils, i.e. that early silicification of microorganisms allows their morphological preservation, the impact of advanced (thermal) diagenesis on the molecular signatures of silicified microorganisms remains to be precisely documented. In fact, this appears as the prerequisite to, eventually, clear the way for the reconstruction of the original chemistry of putative fossilized microorganisms.

Here, we report results of advanced fossilization experiments performed on prokaryotic cyanobacteria *Gloeobacter violaceus* and eukaryotic microalgae *Euglena gracilis* that we experimentally entombed within a silica gel initially consisting of opal-A, i.e. a hydrated amorphous form of silica. Following the philosophy of Oehler (1976a), who performed fossilization experiments under pressure and temperature conditions typical of diagenesis, the present advanced fossilization experiments have been performed at 250 °C and 250 bars for different durations (1, 10 and 100 days) to simulate burial-induced diagenetic processes. These temperature conditions typical of sub-greenschist facies metamorphism are similar to those experienced by most Archean cherts (e.g., Tice et al., 2004; Sugitani et al., 2007, 2010; Glikson et al., 2008; Javaux et al., 2010; Lepot et al., 2013). Regardless its value, pressure is important as it authorizes microtextural transformation (Beyssac et al., 2003). A sample of microorganism-free silica gel and silica-free microorganisms have also been submitted to the same conditions to serve as control groups. Experimental residues have been characterized using X-ray diffraction (XRD) and synchrotron-based X-ray absorption near edge structure (XANES) spectroscopy to document both mineralogical and organic geochemical evolution of these silicified microorganisms. The present results demonstrate that silica restrains the molecular degradation of microorganisms during experimental fossilization at 250 °C and 250 bars and still offers effective protection even after the conversion of silica into quartz. Extrapolating the present results suggests that the mechanism of impeding chemical degradation via silica emplacement may be relevant in fossilization of organic materials over geological timescales.

2. Methods

2.1. Selected microorganisms

Although most experimental silicification studies have been historically performed on cyanobacteria (Oehler and Schopf, 1971; Oehler, 1976a; Walters et al., 1977; Francis et al., 1978a, 1978b; Phoenix et al., 2000; Yee et al., 2003; Benning et al., 2004a; Benning et al., 2004b; Orange et al., 2013a, 2013b), the response to silicification of a wide range of microorganisms has also been investigated, including other bacteria, either Gram-positive (Fortin and Ferris, 1998; Fein et al., 2002; Orange et al., 2014) or Gram-negative (Birnbaum et al., 1989; Fortin and Ferris, 1998; Toporski et al., 2002; Lalonde et al., 2005), archaea and viruses (Orange et al., 2009, 2011a, 2011b, 2012), and eukaryotes (Walters et al., 1977; Francis et al., 1978a, 1978b; Westall et al., 1995).

Here, we selected two strains of unicellular oxygenic photosynthetic microorganisms for advanced fossilization experiments: the prokaryotic cyanobacteria *Gloeobacter violaceus* (PCC 7421) and the eukaryotic microalgae *Euglena gracilis* (n°1224-5d - Cambridge). Fresh *G. violaceus* exhibit purple spherical cells of about 1 μm in diameter, while fresh *E. gracilis* cells are green and approximately 30 μm in length and 10 μm in width (Fig. 1). Obviously, these two strains have not been selected to exemplify all prokaryotic and eukaryotic microorganisms, but rather to serve as two different well-known precursors for the present experiments.

G. violaceus are believed to have diverged phylogenetically prior to the endosymbiotic event responsible for the apparition of the first

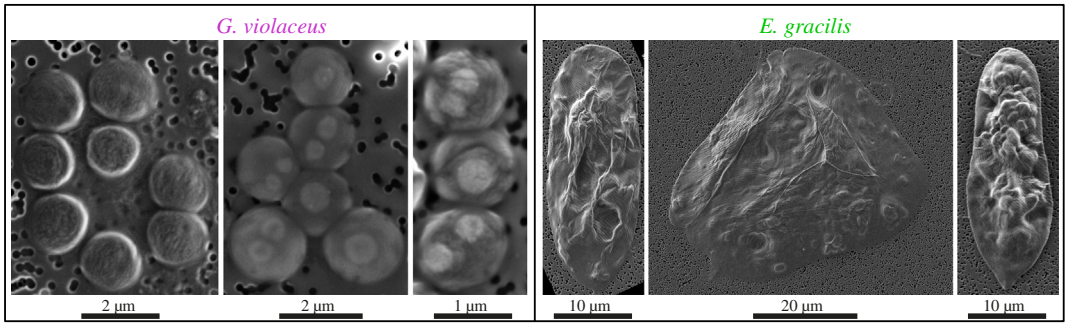

Fig. 1. Scanning electron microscopy observations of the selected microorganisms (*G. violaceus* on the left, *E. gracilis* on the right).

eukaryotic cells (Rexroth et al., 2011). *G. violaceus* produce intracellular Mg-rich polyphosphate vesicles which are used by the cells as a storage form of phosphorus (Benzerara et al., 2014 – Fig. 1). TEM observations of ultrathin sections revealed an atypical cell wall structure compared to other cyanobacteria, comprising, from interior to exterior, an electron-dense peptidoglycan layer which serves a structural role, an intermediate electron-dense cell wall layer, a double track-structured outer membrane, and an adherent external sheath layer (Rippka et al., 1974; Guglielmi et al., 1981; Schneider and Jürgens, 1991). In addition to a peptidoglycan-polysaccharide complex, *Gloeobacter violaceus* contain lipopolysaccharides (20–25wt%), proteins (20–25wt%), carbohydrates (15–20wt%), and fatty acids (2-10wt%) as main constituents of their cell walls (Schneider and Jürgens, 1991).

E. gracilis belong to an ancient lineage near the base of the eukaryotic tree of life and are among the most documented photosynthetic euglenoids (e.g., Cramer and Myers, 1952; Guttman, 1971; Gibbs, 1978; Vismara et al., 2000; Miot et al., 2008, 2009; Leloup et al., 2013; Williams, 2016). These flagellated protists contain chlorophyll-rich chloroplasts which control the synthesis of carbohydrates stored intracellularly as starch granules and paramylon which can reach up to 90% dry weight (Guttman, 1971). Structurally, *E. gracilis* do not have a cell wall, but a pellicle made up of a protein layer supported by a substructure of microtubules arranged in strips spiraling around the cells (Sommer, 1965; Vismara et al., 2000). The complexity of this structure is also reflected in its chemical composition: the pellicle dry weight consists of about 70% of proteins, 15–20% of lipids, and 10–15% of carbohydrates (Barras and Stone, 1965; Nakano et al., 1987).

Both strains have been cultured at IMPMC. *G. violaceus* have been cultured in a regular BG-11 culture medium as done by Couradeau et al. (2012) following the recommendations of the Pasteur institute while *E. gracilis* have been cultured at ambient temperature, under permanent light exposure with ethanol as a carbon source, in a culture medium composed of KH_2PO_4 (0.5 $g \cdot L^{-1}$), $MgSO_4,7H_2O$ (0.5 $g \cdot L^{-1}$), $CaCl_2,2H_2O$ (0.26 $g \cdot L^{-1}$), $(NH_4)2HPO_4$ (0.5 $g \cdot L^{-1}$), a complement of vitamins, zinc (as $ZnSO_4$), iron (as $FeCl_3$), and manganese (as $MnSO_4$) as done by Miot et al. (2008, 2009). Cells of both strains have then been rinsed 3 times in bi-distilled water dried in an oven at 50 °C under vacuum for 3 days.

2.2. Encapsulation within the silica gel and fossilization experiments

Dried micro-organisms have been experimentally entombed within a silica gel following the procedure developed by Nassif et al. (2002). Silica sources were sodium silicate solutions SiNa (27 wt% SiO2, 10 wt% NaOH from Aldrich) and colloidal silica (LUDOX HS-40 from Aldrich). SiNa (0.4 M, 1 mL) has been mixed with LUDOX (8.5 M, 1 mL) and hydrochloric acid (4 M) has been added until neutralization. The mixture has been homogenized under mild stirring before the addition of 1 mL of cyanobacterial or algal suspension (which leads to a final total organic content of the gels of about 5 wt%). Gelation of these mixtures usually occurs within a few minutes at room temperature.

After a 3 day-long drying in an oven at 50 °C under vacuum, 1 mg of microorganism-rich silica gel has been placed into individual gold capsules which have then been sealed under argon atmosphere using an electrical arc and placed in Parr © autoclaves that have been pressurized using argon (>99.99% purity). Pressure has been maintained for all experiments at 250 ± 2.5 bars while temperature has been fixed at 250 ± 2.5 °C using a cylindrical electrical oven. Experiments have been performed over 1, 10 and 100 days, thereby allowing kinetic investigations.

Microorganism-free silica gels and silica-free microorganisms have also been submitted to the same conditions to serve as control groups. All experiments have been repeated three times. At the end of these 1, 10 and 100 day-long experiments, solid residues have been recovered from the capsules and stored at 4 °C before being prepared for XRD and XANES measurements.

2.3. Characterization techniques

2.3.1. X-ray diffraction (XRD)

The bulk mineralogical composition of the experimental products has been determined using a Panalytical X'pert Pro X-ray diffractometer (IMPMC - Paris, France) operating at 40 kV and 40 mA Co Kα radiations. Sample analyses have been carried out on finely ground powders deposited on a silicium sample holder, in the 20°–110° 2θ angle range, with a step size of 0.016° (2θ) for a total counting time per sample of about 6 h. XRD patterns have been analyzed using the Eva software (Bruker) for background subtraction and peak finding.

2.3.2. Scanning Electron Microscopy (SEM)

SEM observations have been performed on pieces of experimental products affixed to aluminum stubs and coated with 15 nm of gold using a SEM-FEG ultra 55 Zeiss (IMPMC - Paris, France) microscope. The operating conditions were as follows: 2 kV accelerating voltage and a working distance of 2 mm for secondary electron imaging (SE2 detector), and 15 kV accelerating voltage and a working distance of 7.5 mm for examination using backscattered electrons (AsB detector).

2.3.3. Synchrotron-based XANES spectroscopy

The 'bulk' carbon speciation of the experimental residues has been investigated by X-ray Absorption Near Edge Structure (XANES) spectroscopy at the carbon *K*-edge (270–330 eV) using the 11-ID-1 Spherical Grating Monochromator (SGM) beamline located at the Canadian Light Source (CLS - Canada) (Regier et al., 2007).

The CLS storage ring is operated at 2.9 GeV and between 250 and 150 mA current. Two horizontal deflecting mirrors and one vertical focusing mirror direct the light from the 45 mm planar undulator through the entrance slit and onto a 1700 lines/mm grating (low energy grating) which diffracts the light through a movable exit slit that has been set at 15 μm for the present experiments. A pair of toroidal refocusing mirrors are used to focus the beam onto the samples in the endstation chamber maintained at a pressure of about 10^{-7} Torr. A 100 nm thick titanium filter is used to remove the contribution of second order light.

The beam spot size is approximately 1 mm × 100 μm with a flux (normalized to 100 mA) greater than 10^{12} photons at 250 eV. This beamline measures the fluorescence yield of samples exposed to the incident beam as a function of its energy with a spectral resolution of about 0.1 eV. When normalized to the scattering intensity from a clean gold foil used as a blank, fluorescence yields are directly comparable to absorption data, especially as the SGM uses an Amptek silicon drift detector placed at exactly 90° to the incident beam, a configuration which allows exclusion of the scattered light.

Experimental residues have been pressed onto gold foils (99.99% purity - Sigma Aldrich) then mounted on a copper sample holder. Calibration in energy has been done using a set of pure reference materials (calcium carbonate, benzoic acid and histidine (>99% purity - Sigma Aldrich)). Each spectrum reported in the present study corresponds to the average of about 50 measurements collected at different locations over the sample surfaces. Of note, only the first 100 nm of the sample surface are probed using the SGM setup. Spectra have been averaged, background subtracted and normalized using the Igor Pro software.

2.4. XANES data deconvolution procedure

C-XANES spectroscopy has been successfully used to document the carbon speciation of organic microfossils (Bernard et al., 2007, 2009; Lepot et al., 2008, 2009; De Gregorio et al., 2009, 2011; Cosmidis et al., 2013a, 2013b; Robin et al., 2015; Alleon et al., 2016). Absorption peaks of a C-XANES spectrum constitute sensitive indicators of the local chemical bonding environment surrounding the carbon atoms and correspond to transitions from core shell (1s) electrons to both unoccupied π* (antibonding) and low lying σ* orbitals.

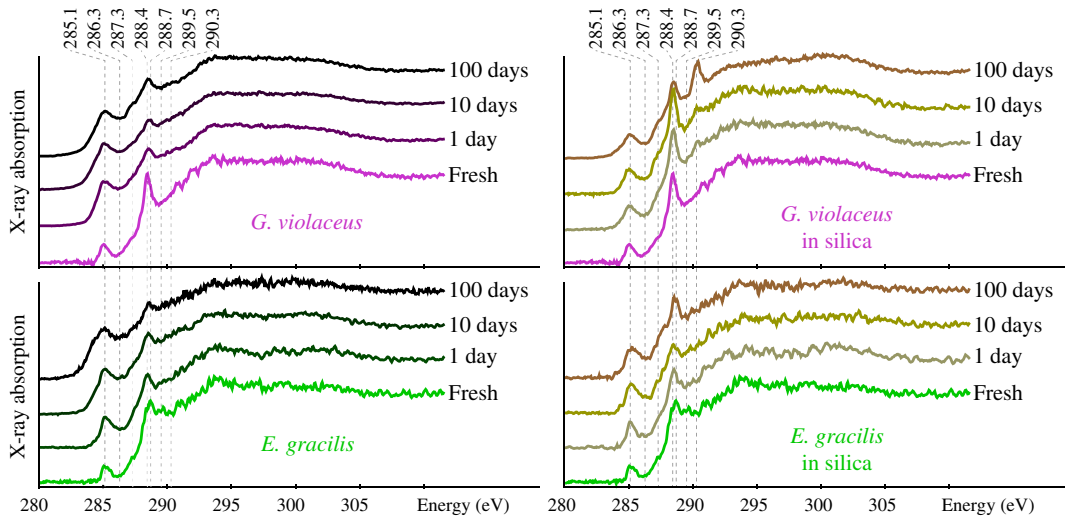

Fig 2. X-ray absorption near edge structure spectra of experimental residues. C-XANES spectra collected on the starting materials and on the residues of *G. violaceus* (top) and *E. gracilis* (bottom) experimentally fossilized under 250 °C and 250 bars for 1, 10 and 100 days in the absence of silica (left) and entombed in silica (right). Peak attribution: 285.1 eV: aromatic; 287.3 eV: carbonyl/phenol; 288.4 eV: amide + carboxyl/ester/acetal; 288.7 eV: carboxyl/ester/acetal; 289.5 eV: hydroxyl; 290.3 eV: carbonate.

As any electric-dipole transition spectroscopies, XANES spectroscopy adheres to Beer's law. Variations in peak intensities are thus directly proportional to variations in concentration of the absorbing functional groups. Assuming that the oscillator strength of a given functional group is essentially the same in organic compounds of similar chemistry (Ishii and Hitchcook, 1988; Francis and Hitchcock, 1992), the relative concentrations of the different functional groups for the residues investigated can be discussed qualitatively.

To obtain a more quantitative insight on the molecular signatures of the experimental samples investigated, the C-XANES spectra normalized to the total carbon amount (measured above 320 eV) have been deconvolved using the Athena software package (Ravel and Newville, 2005) following the procedure described by Bernard et al. (2015), based on the recommendations of Braun et al. (2006).

The absorption edge itself has been modeled using an arctangent function which center position, amplitude and width at half-height have been fixed to 291.5 eV, 1.0, and 0.4 eV, respectively. The remaining absorption signal has been fitted using Gaussian functions, each of them having a fixed energy position and a constant width (0.4 eV below 295 eV and 2 eV above).

Although the natural lineshape of a XANES peak is a Lorentzian function, Gaussian functions have been used to take into account the contribution of instrumental broadening effects. It should be kept in mind that most of the Gaussian functions used for these deconvolutions do not account for the presence of functional groups but for broad spectral features corresponding to highly delocalized excited states, sometimes referred to as 1s → σ* virtual state transitions, or for the overlapping contribution of Feshbach resonances.

The normalized 'aromaticity index' is defined here as the sum of the areas of the Gaussian functions accounting for the absorption related to the presence of multiple carbon-carbon bond species and used to deconvolve the broad peak at 285 eV according to Bernard et al. (2010c, 2015) and Le Guillou et al. (2013, 2014), normalized, for each strain, to the aromaticity index of the starting material.

3. Results

The C-XANES spectrum of fresh *G. violaceus* is typical of bacteria (Fig. 2), with a main peak at 288.4 eV, attributed to the joint contributions of 1s → π* electronic transitions in amide groups (occurring at 288.2 eV) and of 1s → π* electronic transitions in carboxylic (COOH), ester (COOR) or acetal ($C(OR)_2$) groups (occurring at 288.5–288.7 eV), a peak at 285.1 eV, attributed to 1s → π* electronic transitions in aromatic or olefinic groups (C═C), and a shoulder centered at about 287.3 eV,

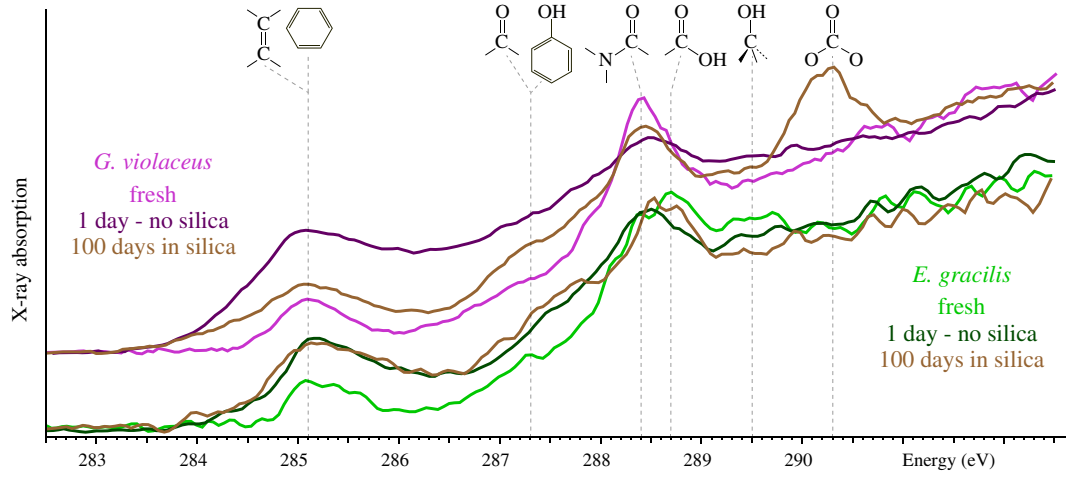

Fig. 3. X-ray absorption near edge structure spectra of experimental residues. C-XANES spectra of *G. violaceus* and *E. gracilis* experimentally fossilized under 250 °C and 250 bars for 100 days entombed in silica and for 1 day in the absence of silica. C-XANES spectra of starting materials are shown for comparison.

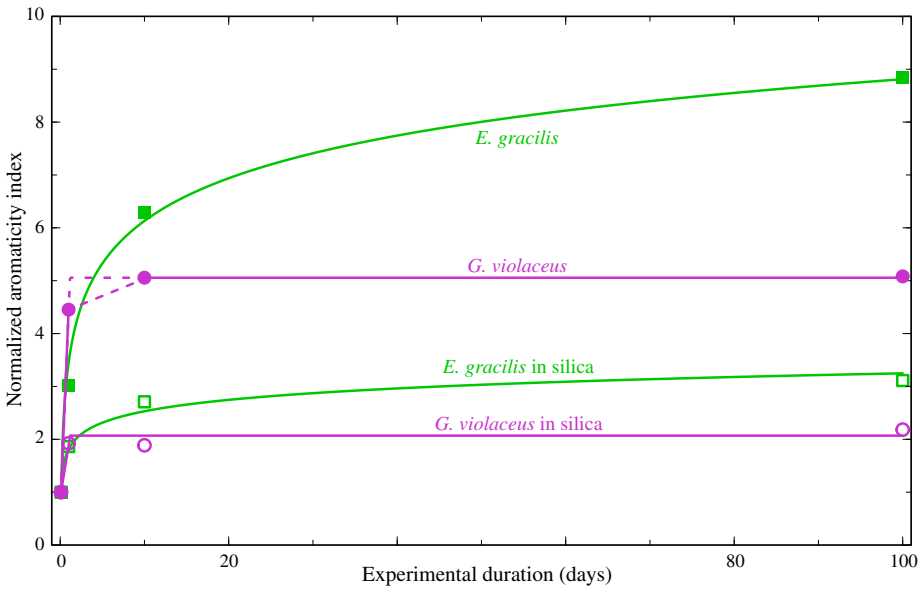

Fig. 4. Evolution of the aromaticity index of experimental residues. Aromaticity indexes of *G. violaceus* (circles) and *E. gracilis* (squares) experimentally fossilized under 250 °C and 250 bars for 1, 10 and 100 days in the absence of silica (open symbols) and entombed in silica (filled symbols). Logarithmic curves are used to fit the data for *E. gracilis* only (see text for details).

attributed to 1s → π* electronic transitions in carbonyl (C═O) and phenolic (Ar-OH) groups (Benzerara et al., 2006; Solomon et al., 2009; Li et al., 2014). This spectrum is consistent with the initial composition of *G. violaceus* cell walls (Schneider and Jürgens, 1991).

The C-XANES spectrum of fresh *E. gracilis* appears slightly different (Fig. 2). In fact, it also exhibits an absorption feature at 289.5 eV corresponding to 1s → 3p/σ* transitions in hydroxyl functional groups (Cody et al., 2011; Bernard et al., 2012a, 2012b). In addition, instead of being centered at 288.4 eV, its intense peak is centered at 288.7 eV and can be attributed to 1s → π* transitions in carboxylic groups (COOH), ester (COOR) or acetal groups ($C(OR)_2$) (Johansson and Campbell, 2004; Bernard et al., 2012a, 2012b; Rouchon and Bernard, 2015). These contributions are likely related to a high content of carbohydrates (Lawrence et al., 2003), which, in the case of *E. gracilis*, are stored intracellularly as starch granules and paramylon (Guttman, 1971).

In the absence of silica, *G. violaceus* and *E. gracilis* have evolved towards dark oily residues with no specific morphologies during experimental fossilization at 250 °C and 250 bars, even after only one day. The C-XANES spectra of the experimental residues reveal that *G. violaceus* and *E. gracilis* have encountered a significant chemical evolution (Fig. 2). For both strains, the relative concentrations of aromatic/olefinic carbons and carbonyl/phenolic carbons have significantly increased (absorption features at 285.1 and 287.3 eV have become more intense) while the relative concentrations of amide/acetal/carboxylic and hydroxylated carbons have significantly decreased (intensities of absorption peaks at 288.4/288.7 and 289.5 eV have decreased) after only one day. While the molecular degradation of *G. violaceus* seems to be complete after 1 day, the molecular signature of *E. gracilis* has evolved more progressively with increasing experimental duration (Fig. 2).

The molecular signatures of *G. violaceus* and *E. gracilis* entombed in silica and submitted to experimental fossilization under the same conditions have evolved following similar trends, i.e. *E. gracilis* have evolved more progressively than *G. violaceus*. Yet, little or no oil has formed from microorganisms entombed in silica and the transformations encountered by these microorganisms appear significantly less drastic than the ones they have encountered in the absence of silica (Figs. 2 and 3). In particular, *G. violaceus* entombed in silica still contain amide groups after 100 days. Interestingly, the C-XANES spectra of the residues of *G. violaceus* entombed in silica exhibit an additional absorption feature at 290.3 eV which can be attributed to 1s → π* transitions in carbonate groups (Benzerara et al., 2006; Brandes et al., 2010), which increases in intensity with increasing experimental duration from 1 to 100 days. These carbonates may result from the destabilization of intracellular polyphosphates during the experiments.

Following previous studies (Bernard et al., 2010c, 2015; Le Guillou et al., 2013, 2014), the 'aromaticity index' of *G. violaceus* and *E. gracilis* has been extracted from C-XANES data. An increase of the aromaticity index indicates an increase of maturity, *i.e.* a degradation of the initial molecular composition. For each strain, the aromaticity index of the residues of experiments performed in silica is significantly lower than that of experiments performed in the absence of silica (Fig. 4). Intriguingly, independent of the presence or absence of silica, the aromaticity index of the residues of *G. violaceus* is always lower than that of *E. gracilis* for a given experimental duration. In addition, for *G. violaceus*, this index increases during the first day and does not significantly vary for longer exposure. In contrast, the aromaticity index of *E. gracilis* exhibits a log-linear relationship with experimental duration (Fig. 4).

The silica gels in which the microorganisms investigated have been entombed consist of opal-A, a hydrated amorphous form of silica, as indicated by XRD (Fig. 5). In the absence of microorganisms, the silica gel is converted into quartz in less than a day when submitted to 250 °C and 250 bars (Fig. 5). The silica gel originally containing *G. violaceus* has also rapidly crystallized into quartz (in less than a day) while the silica gel originally containing *E. gracilis* has remained amorphous during the first day and evolved towards opal-CT in the 10 day-long experiments to become an assemblage of opal-C and quartz with increasing experimental duration (Fig. 5).

SEM observations of residues of experiments performed on microorganisms entombed in silica reveal that organics have been redistributed within the mineral matrix, even after the shortest (1 day-long) experiments (Fig. 6). Within the samples originally containing *G. violaceus*, empty silica lepispheres have rapidly formed (in less than a day). The formation of similar silica lepispheres appears more progressive within the samples originally containing *E. gracilis* (Fig. 6).

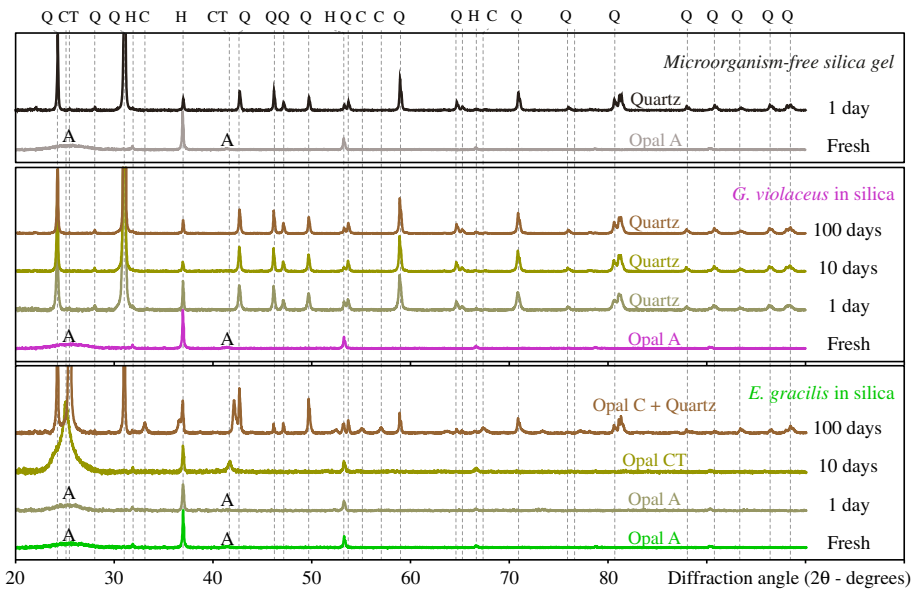

Fig. 5. X-ray diffraction patterns of experimental residues. XRD patterns of the silica matrix of the starting materials and of the residues of *G. violaceus* (middle) and *E. gracilis* (bottom) experimentally entombed in silica and submitted to 250 °C and 250 bars for 1, 10 and 100 days. Opal-A (A), opal-CT (CT), opal-C (C), quartz (Q) and halite (H) are indexed. Also shown are the XRD patterns of the microorganism-free silica gel before and after experimental fossilization 250 °C and 250 bars for 1 day (top).

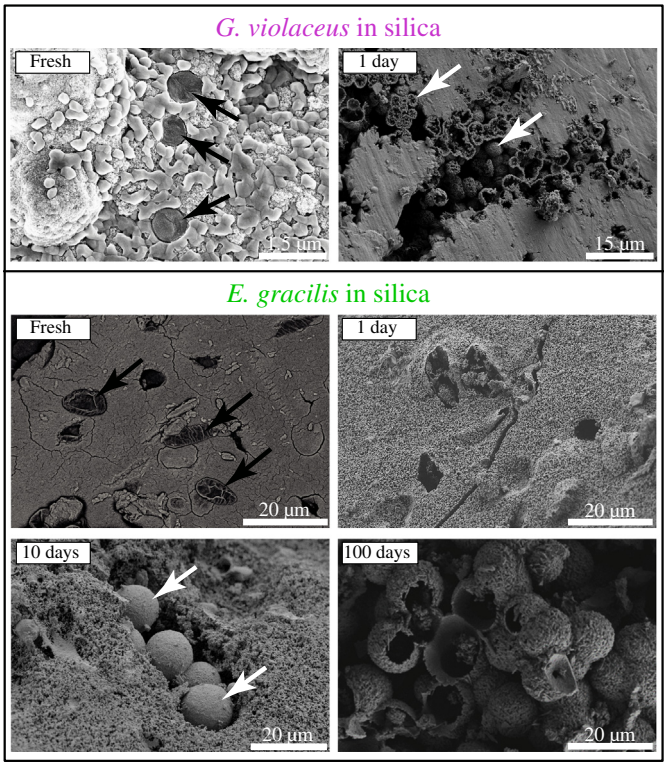

Fig. 6. Scanning electron microscopy observations of experimental residues. SEM images (secondary electrons) of the starting materials and of the residues of *G. violaceus* (top) and *E. gracilis* (bottom) experimentally entombed in silica and submitted to 250 °C and 250 bars for 1, 10 and 100 days. Black arrows show the microorganisms freshly entombed in the silica gel. White arrows show the silica spheres (lepispheres) formed during the fossilization experiments.

4. Discussion

4.1. Degradation of microorganisms

The present study provides experimental insights on burial-induced microorganism degradation processes from a molecular point of view. In the absence of silica, the evolution towards dark oily residues of *G. violaceus* and *E. gracilis* likely indicates oil and bitumen generation through thermal cracking reactions (Dieckmann et al., 1998; Behar et al., 1997; Lewan, 1997; Behar et al., 2003; Lewan and Roy, 2011; Bernard and Horsfield, 2014) and a concomitant increase of aromaticity of the solid residue (Hartkopf-Fröder et al., 2015). C-XANES data reveal that the evolution of *G. violaceus* and *E. gracilis* is typical of organic solids having experienced thermal maturation (Schiffbauer et al., 2012; Li et al., 2014; Bernard et al., 2015), i.e. a loss of oxygen-containing functional groups concomitant to an increase of the relative abundance of aromatic structures (e.g., Bernard and Horsfield, 2014). For both strains, the absence of a sharp $1s \rightarrow \sigma^*$ exciton at 291.7 eV, related to the presence of extensive planar domains of highly conjugated aromatic layers (Cody et al., 2008; Bernard et al., 2010c), suggests that significant pericondensation of aromatic rings has not occurred even after 100 days.

Intriguingly, the aromaticity index of *E. gracilis* exhibits a log-linear relationship with experimental duration which does not correspond to any reaction mechanism commonly operating in solid/solid organic reactions (Rothenberg et al., 2001). Similar log-linear behaviors have been reported for parameters describing the maturation/degradation of carbon materials as a function of experiment durations (Beyssac et al., 2003; Cody et al., 2008; Zhao et al., 2010; Schiffbauer et al., 2012; Bernard et al., 2015). This behavior suggests that the degradation of *E. gracilis* has mainly occurred through a series of kinetically controlled reactions such as, for instance, random chain scissions and polymerization/condensation reactions (Rothenberg et al., 2001; Vandenbroucke and Largeau, 2007; Sánchez-Jiménez et al., 2010; Pérez-Maqueda et al., 2014). Of note, this apparent log-linear kinetic behavior likely turns into a plateau when a thermodynamic metastable equilibrium is reached as it is likely the case in natural settings (Helgeson et al., 1993, 2009; Richard and Helgeson, 1998).

In contrast to *E. gracilis*, the aromaticity index of *G. violaceus* residues does not continue to evolve after the first day of experiment. This implies that either the aromaticity increase of *G. violaceus* residues has

not followed a log-linear kinetic behavior or that a log-linear relationship has turned into a plateau in less than a day. Such different behavior between *G. violaceus* and *E. gracilis* might be a result of the high carbohydrate concentration of *E. gracilis*. In fact, acetal functional groups, abundant in carbohydrates, are known to be more resistant to thermal degradation processes than amide functional groups (Vandenbroucke and Largeau, 2007). In any case, the present results evidence that slightly different organics may follow significantly different degradation pathways during advanced (thermal) diagenesis.

4.2. Influence of the silica matrix

The present experimental results demonstrate that entombment within silica limits the molecular degradation of microorganisms. The opposite could have been expected as the silica matrix used for the present experiments mainly consists of hydrated opal-A. In fact, the presence of water has been shown to enhance organic maturation processes as well as oil and bitumen generation at low-temperature (Lewan, 1997; Behar et al., 2003; Lewan and Roy, 2011). Here, despite the high water content of the silica matrix, the C-XANES spectrum of *E. gracilis* entombed in silica and submitted to 250 °C and 250 bars for 100 days appears very similar to the C-XANES spectrum of *E. gracilis* submitted to the same conditions for only 1 day in the absence of silica (Fig. 3). The preservation of *G. violaceus* entombed in silica is even more remarkable (Fig. 3).

Such molecular preservation likely results from specific chemical interactions between the investigated microorganisms and the silica matrix, as historically proposed to explain the fine-scale morphological preservation of silicified wood (Leo and Barghoorn, 1976). Amino acids and peptides can interact with silica-rich solutions through electrostatic interactions and hydrogen bonding (Coradin and Livage, 2001; Benning et al., 2004a, 2004b; Konhauser et al., 2004). Hydroxyl-bearing functional groups of organic molecules can be adsorbed through hydrogen bonding with silanols (Hsu et al., 2000; Coradin and Livage, 2001; Jal et al., 2004; Konhauser et al., 2004; Zou et al., 2008; Ciriminna et al., 2013). The concentration of silanols at the surface of silica is directly related to its degree of hydration (Zhuravlev, 2000; Konecny, 2001). Si—O—C covalent bonds may form during water release, resulting in the stabilization of some organic functional groups despite increasing temperature conditions (Hsu et al., 2000; Jal et al., 2004; Zou et al., 2008). Such stabilization has likely limited oil and bitumen generation through thermal cracking reactions (little or no oil has formed during the experiments with silica) and thereby having restricted the aromatization of organic residues.

Although it remains significantly lower, the aromaticity indices of *E. gracilis* and *G. violaceus* entombed in silica exhibit similar relationship with experimental duration to those of *E. gracilis* and *G. violaceus* experimentally fossilized in the absence of silica, respectively. In other words, *G. violaceus* and *E. gracilis* entombed in silica exhibit degradation patterns similar to those observed for experiments performed in the absence of silica. The present study thus pinpoints that, even within silica, the molecular signatures of different organic precursors may follow different degradation pathways.

Of note, despite previous observations of silicification preserving microbial morphologies (Oehler and Schopf, 1971; Oehler, 1976a; Walters et al., 1977; Francis et al., 1978a, 1978b; Birnbaum et al., 1989; Westall et al., 1995; Phoenix et al., 2000; Toporski et al., 2002; Lalonde et al., 2005; Orange et al., 2009, 2011a, 2011b, 2012, 2013a, 2013b, 2014), entombment within silica has not promoted the morphological preservation of *G. violaceus* and *E. gracilis* cells during the present experiments. The present closed-system experimental design may have precluded the escape of volatile products, thus promoting the circulation of fluids and the scatter of organics within the silica matrix. The empty molds resulting from the migration of organics likely served as templates for the formation of silica lepispheres similar to those formed in natural silica sinters (Flörke et al., 1976; Rimstidt and Cole, 1983; Herdianita et al., 2000; Rodgers et al., 2004; Lynne et al., 2005).

4.3. Evolution of the silica matrix

The silica gel originally consisting of hydrated opal-A has evolved towards opal-CT, opal-C and quartz during the fossilization experiments with *E. gracilis*. Similar mineralogical changes accompany ageing of silica sinters in natural settings (Flörke et al., 1976; Rimstidt and Cole, 1983; Herdianita et al., 2000; Rodgers et al., 2004; Lynne et al., 2005). Interestingly, the evolution of the silica matrix of samples containing microorganisms seems closely related to (if not controlled by) the evolution/degradation of the entombed microorganisms. Silica crystallization has indeed been more progressive in samples containing *E. gracilis* compared to samples containing *G. violaceus*, i.e. silica crystallization patterns are similar to the molecular degradation patterns of *E. gracilis* and *G. violaceus*.

In the absence of microorganisms, the silica gel is converted into quartz in less than a day when submitted to 250 °C and 250 bars, in good agreement with previous experiments performed under similar conditions (Corwin et al., 1953; Bettermann and Liebau, 1975; Oehler, 1976b; Kastner et al., 1977; Hinman, 1990; Okamoto et al., 2010). As it is also the case in the presence of *G. violaceus*, it is difficult to infer if/how the presence of cyanobacteria has impacted the crystallization of the silica gel. The transition from opal to quartz has been shown to be faster in the presence of ions such as Mg^{2+} (Kastner et al., 1977; Kyle and Schroeder, 2007) or minerals such as carbonates (Kastner et al., 1977; Hinman, 1990; Herdianita et al., 2000; Rodgers et al., 2004; Lynne et al., 2005; Lakshtanov and Stipp, 2010). As the intracellular Mg-rich polyphosphate vesicles of *G. violaceus* have decomposed into carbonates during the experiments, the presence of *G. violaceus* may have slightly accelerated the crystallization of the silica gel.

In contrast, the XRD data reported here evidence that the presence of *E. gracilis* has retarded the crystallization of the silica gel. Although organics have only little affinity for monomeric silica, their presence may affect the crystallization rate of amorphous silica and, depending on their chemical composition, impart an influence on the fabric of silica sinters (Hinman, 1990; Fein et al., 2002; Yee et al., 2003; Konhauser et al., 2004; Rodgers et al., 2004; Handley et al., 2008). Previous observations on natural samples have similarly suggested that chemical interactions between organics and silica may hinder crystallization processes (Moreau and Sharp, 2004; Foucher and Westall, 2013). As hydrogen bonds between amorphous silica and organics mainly occur with hydroxyl-bearing functional groups (Hsu et al., 2000; Coradin and Livage, 2001; Jal et al., 2004; Konhauser et al., 2004; Zou et al., 2008; Ciriminna et al., 2013), silica crystallization has likely been retarded in the present experiments because of the high quantity of hydroxyl-rich carbohydrates formed intracellularly by *E. gracilis*.

5. Concluding remarks: significance for natural settings

Extrapolating laboratory results to natural settings remains difficult, notably because geological timescales cannot be replicated in the laboratory (Li et al., 2014; Bernard et al., 2015; Picard et al., 2015a, 2015b). Nevertheless, similar to what occurs in natural silica sinters (Flörke et al., 1976; Rimstidt and Cole, 1983; Herdianita et al., 2000; Rodgers et al., 2004; Lynne et al., 2005), quartz has become the main constituent of all residues of 100 day long experiments. Although quartz surfaces are less hydroxylated than other polymorphs of silica (Zhuravlev, 2000; Konecny, 2001), the microorganisms used for the present fossilization experiments seem to have encountered only limited molecular degradation between 10 and 100 days, suggesting that organics and silica are mostly associated through covalent bonds after the first 10 days of experiment. The present degradation patterns of *G. violaceus* and *E. gracilis* thus suggest that their molecular signatures could still be (at

least partially) preserved even after much longer exposures to such diagenetic conditions.

Although the present experimental results hold great promise for the detection of (partially) preserved molecular signatures of ancient organic microfossils, additional experimental studies appear necessary to thoroughly constrain the molecular evolution of biogenic organic molecules during burial-induced processes and eventually reconstruct the original chemical composition of fossilized microorganisms. In fact, neither biodegradation nor early taphonomic processes that usually occur in natural settings have been simulated here. In addition, quartz may crystallize at lower temperatures, thereby modifying silica-organics interactions. A possible way to overcome this obstacle would be to submit well-characterized, already indurated sedimentary rocks to experimental fossilization. This would allow more accurately simulating natural processes and hence obtaining a more realistic view of the chemical evolution that may have experienced ancient microorganisms during burial processes.

Acknowledgments

We gratefully acknowledge support from the ERC (project PaleoNanoLife - PI: F. Robert) (grant #161764). Special thanks go to Mélinée Deretz for administrative simplification. The SEM facility of the IMPMC is supported by Région Ile de France grant SESAME 2006 N °I-07-593/R, INSU-CNRS, INP-CNRS, UPMC-Paris 6, and by the Agence Nationale de la Recherche (ANR) grant No. ANR-07-BLAN-0124-01. Special thanks go to Imene Esteve for her expert support of the SEM at IMPMC. Bulk XANES data were acquired at beamline 11ID-1 at the CLS, which is supported by the NSERC, the CIHR, the NRC, and the University of Saskatchewan. Special thanks go to Tom Regier and Jay Dynes for their expert support of the SGM beamline.

References

Alleon, J., Bernard, S., Le Guillou, C., Marin-Carbonne, J., Pont, S., Beyssac, O., McKeegan, K.D., Robert, F., 2016. Molecular preservation of 1.88 Ga Gunflint organic microfossils as a function of temperature and mineralogy. Nat. Commun. 7, 11977. http://dx.doi.org/10.1038/ncomms11977.

Anderson, E.P., Schiffbauer, J.D., Xiao, S., 2011. Taphonomic study of Ediacaran organic-walled fossils confirms the importance of clay minerals and pyrite in Burgess Shale-type preservation. Geology 39 (7), 643–646. http://dx.doi.org/10.1130/G31969.1.

Barras, D.R., Stone, B.A., 1965. The chemical composition of the pellicle of *Euglena gracilis var. bacillaris*. Biochem. J. 97 (2), 14–15.

Behar, F., Lewan, M.D., Lorant, F., Vandenbroucke, M., 2003. Comparison of artificial maturation of lignite in hydrous and nonhydrous conditions. Org. Geochem. 34 (4), 575–600. http://dx.doi.org/10.1016/S0146-6380(02)00241-3.

Behar, F., Vandenbroucke, M., Tang, Y., Marquis, F., Espitalie, J., 1997. Thermal cracking of kerogen in open and closed systems: determination of kinetic parameters and stoichiometric coefficients for oil and gas generation. Org. Geochem. 26 (5), 321–339. http://dx.doi.org/10.1016/S0146-6380(97)00014-4.

Benning, L.G., Phoenix, V.R., Yee, N., Konhauser, K.O., 2004b. The dynamics of cyanobacterial silicification: an infrared micro-spectroscopic investigation. Geochim. Cosmochim. Acta 68 (4), 743–757. http://dx.doi.org/10.1016/S0016-7037(03)00488-5.

Benning, L.G., Phoenix, V.R., Yee, N., Tobin, M.J., 2004a. Molecular characterization of cyanobacterial silicification using synchrotron infrared micro-spectroscopy. Geochim. Cosmochim. Acta 68 (4), 729–741. http://dx.doi.org/10.1016/S0016-7037(03)00489-7.

Benzerara, K., Menguy, N., López-García, P., Yoon, T.H., Kazmierczak, J., Tyliszczak, T., Guyot, F., Brown, G.E., 2006. Nanoscale detection of organic signatures in carbonate microbialites. Proc. Natl. Acad. Sci. 103 (25), 9440–9445. http://dx.doi.org/10.1073/pnas.0603255103.

Benzerara, K., Skouri-Panet, F., Li, J., Férard, C., Gugger, M., Laurent, T., Couradeau, E., Ragon, M., Cosmidis, J., Menguy, N., Margaret-Oliver, I., Tavera, R., López-García, P., Moreira, D., 2014. Intracellular Ca-carbonate biomineralization is widespread in cyanobacteria. Proc. Natl. Acad. Sci. 111 (30), 10933–10938. http://dx.doi.org/10.1073/pnas.1403510111.

Bernard, S., Horsfield, B., 2014. Thermal maturation of gas shale systems. Annu. Rev. Earth Planet. Sci. 42, 635–651. http://dx.doi.org/10.1146/annurev-earth-060313-054850.

Bernard, S., Papineau, D., 2014. Graphitic carbons and biosignatures. Elements 10 (6), 435–440. http://dx.doi.org/10.2113/gselements.10.6.435.

Bernard, S., Benzerara, K., Beyssac, O., Balan, E., Brown Jr., G.E., 2015. Evolution of the macromolecular structure of sporopollenin during thermal degradation. Heliyon 1 (2), e00034. http://dx.doi.org/10.1016/j.heliyon.2015.e00034.

Bernard, S., Benzerara, K., Beyssac, O., Brown, G.E., 2010a. Multiscale characterization of pyritized plant tissues in blueschist facies metamorphic rocks. Geochim. Cosmochim. Acta 74 (17), 5054–5068. http://dx.doi.org/10.1016/j.gca.2010.06.011.

Bernard, S., Benzerara, K., Beyssac, O., Brown, G.E., Stamm, L.G., Duringer, P., 2009. Ultrastructural and chemical study of modern and fossil sporoderms by Scanning Transmission X-ray Microscopy (STXM). Rev. Palaeobot. Palynol. 156 (1), 248–261. http://dx.doi.org/10.1016/j.revpalbo.2008.09.002.

Bernard, S., Benzerara, K., Beyssac, O., Menguy, N., Guyot, F., Brown, G.E., Goffé, B., 2007. Exceptional preservation of fossil plant spores in high-pressure metamorphic rocks. Earth Planet. Sci. Lett. 262 (1), 257–272. http://dx.doi.org/10.1016/j.epsl.2007.07.041.

Bernard, S., Beyssac, O., Benzerara, K., Findling, N., Tzvetkov, G., Brown, G.E., 2010b. XANES, Raman and XRD study of anthracene-based cokes and saccharose-based chars submitted to high-temperature pyrolysis. Carbon 48 (9), 2506–2516. http://dx.doi.org/10.1016/j.carbon.2010.03.024.

Bernard, S., Horsfield, B., Schulz, H.-M., Schreiber, A., Wirth, R., Vu, T.T.A., Perssen, F., Könitzer, S., Volk, H., Sherwood, N., Fuentes, D., 2010c. Multi-scale detection of organic and inorganic signatures provides insights into gas shale properties and evolution. Chemie der Erde – Geochemistry 70 (S3), 119–133. http://dx.doi.org/10.1016/j.chemer.2010.05.005.

Bernard, S., Horsfield, B., Schulz, H.M., Wirth, R., Schreiber, A., Sherwood, N., 2012a. Geochemical evolution of organic-rich shales with increasing maturity: a STXM and TEM study of the Posidonia Shale (Lower Toarcian, northern Germany). Mar. Pet. Geol. 31 (1), 70–89. http://dx.doi.org/10.1016/j.marpetgeo.2011.05.010.

Bernard, S., Wirth, R., Schreiber, A., Schulz, H.M., Horsfield, B., 2012b. Formation of nanoporous pyrobitumen residues during maturation of the Barnett Shale (Fort Worth Basin). Int. J. Coal Geol. 103, 3–11. http://dx.doi.org/10.1016/j.coal.2012.04.010.

Bettermann, P., Liebau, F., 1975. The transformation of amorphous silica to crystalline silica under hydrothermal conditions. Contrib. Mineral. Petrol. 53 (1), 25–36. http://dx.doi.org/10.1007/BF00402452.

Beyssac, O., Brunet, F., Petitet, J.P., Goffé, B., Rouzaud, J.N., 2003. Experimental study of the microtextural and structural transformations of carbonaceous materials under pressure and temperature. Eur. J. Mineral. 15 (6), 937–951. http://dx.doi.org/10.1127/0935-1221/2003/0015-0937.

Birnbaum, S.J., Wireman, J.W., Borowski, R., 1989. Silica precipitation induced by the anaerobic sulfate reducing bacterium *Desulfovibrio desulfuricans*: effects upon cell morphology and implications for preservation. Origin, Evolution, and Modern Aspects of Biomineralization in Plants and Animals. Springer, US, pp. 507–516 http://dx.doi.org/10.1007/978-1-4757-6114-6-39.

Brandes, J.A., Wirick, S., Jacobsen, C., 2010. Carbon K-edge spectra of carbonate minerals. J. Synchrotron Radiat. 17 (5), 676–682. http://dx.doi.org/10.1107/S0909049510020029.

Brasier, M.D., Antcliffe, J., Saunders, M., Wacey, D., 2015. Changing the picture of Earth's earliest fossils (3.5–1.9 Ga) with new approaches and new discoveries. Proc. Natl. Acad. Sci. 112 (16), 4859–4864. http://dx.doi.org/10.1073/pnas.1405338111.

Brasier, M.D., Green, O.R., Jephcoat, A.P., Kleppe, A.K., Van Kranendonk, M.J., Lindsay, J.F., Steele, A., Grassineau, N.V., 2002. Questioning the evidence for Earth's oldest fossils. Nature 416 (6876), 76–81. http://dx.doi.org/10.1038/416076a.

Braun, A., Huggins, F.E., Kelly, K.E., Mun, B.S., Ehrlich, S.N., Huffman, G.P., 2006. Impact of ferrocene on the structure of diesel exhaust soot as probed with wide-angle X-ray scattering and C (1s) NEXAFS spectroscopy. Carbon 44 (14), 2904–2911. http://dx.doi.org/10.1016/j.carbon.2006.05.051.

Briggs, D.E., 2003. The role of decay and mineralization in the preservation of soft-bodied fossils. Annu. Rev. Earth Planet. Sci. 31 (1), 275–301. http://dx.doi.org/10.1146/annurev.earth.31.100901.144746.

Briggs, D.E., Kear, A.J., 1993. Fossilization of soft tissue in the laboratory. Science 259 (5100), 1439–1442. http://dx.doi.org/10.1126/science.259.5100.1439.

Briggs, D.E., Summons, R.E., 2014. Ancient biomolecules: their origins, fossilization, and role in revealing the history of life. BioEssays 36 (5), 482–490. http://dx.doi.org/10.1002/bies.201400010.

Briggs, D.E., Wilby, P.R., 1996. The role of the calcium carbonate-calcium phosphate switch in the mineralization of soft-bodied fossils. J. Geol. Soc. 153 (5), 665–668. http://dx.doi.org/10.1144/gsjgs.153.5.0665.

Briggs, D.E.G., Kear, A.J., Martill, D.M., Wilby, P.R., 1993. Phosphatization of soft-tissue in experiments and fossils. J. Geol. Soc. 150 (6), 1035–1038. http://dx.doi.org/10.1144/gsjgs.150.6.1035.

Broce, J., Schiffbauer, J.D., Sharma, K.S., Wang, G., Xiao, S., 2014. Possible animal embryos from the lower Cambrian (stage 3) Shuijingtuo Formation, Hubei Province, South China. J. Paleontol. 88 (2), 385–394. http://dx.doi.org/10.1666/13-062.

Butterfield, N.J., 2003. Exceptional fossil preservation and the Cambrian Explosion. Integr. Comp. Biol. 43 (1), 166–177. http://dx.doi.org/10.1093/icb/43.1.166.

Cady, S.L., Farmer, J.D., 1996. Fossilization processes in siliceous thermal springs: trends in preservation along thermal gradients. Ciba Foundation Symposium. Vol. 202, pp. 150–170.

Campbell, K.A., Lynne, B.Y., Handley, K.M., Jordan, S., Farmer, J.D., Guido, D.M., Foucher, F., Turner, S., Perry, R.S., 2015. Tracing biosignature preservation of geothermally silicified microbial textures into the geological record. Astrobiology 15 (10), 858–882. http://dx.doi.org/10.1089/ast.2015.1307.

Ciriminna, R., Fidalgo, A., Pandarus, V., Béland, F., Ilharco, L.M., Pagliaro, M., 2013. The sol–gel route to advanced silica-based materials and recent applications. Chem. Rev. 113 (8), 6592–6620. http://dx.doi.org/10.1021/cr300399c.

Cody, G.D., Alexander, C.O.D., Yabuta, H., Kilcoyne, A.L.D., Araki, T., Ade, H., ... Mysen, B.O., 2008. Organic thermometry for chondritic parent bodies. Earth Planet. Sci. Lett. 272 (1), 446–455. http://dx.doi.org/10.1016/j.epsl.2008.05.008.

Cody, G.D., Heying, E., Alexander, C.M., Nittler, L.R., Kilcoyne, A.D., Sandford, S.A., Stroud, R.M., 2011. Establishing a molecular relationship between chondritic and cometary

organic solids. Proc. Natl. Acad. Sci. 108 (48), 19171–19176. http://dx.doi.org/10.1073/pnas.1015913108.
Coradin, T., Livage, J., 2001. Effect of some amino acids and peptides on silicic acid polymerization. Colloids Surf. B: Biointerfaces 21 (4), 329–336. http://dx.doi.org/10.1016/S0927-7765(01)00143-6.
Corwin, J.F., Herzog, A.H., Owen, G.E., Yalman, R.G., Swinnerton, A.C., 1953. The mechanism of the hydrothermal transformation of silica glass to quartz under isothermal conditions. J. Am. Chem. Soc. 75 (16), 3933–3934. http://dx.doi.org/10.1021/ja01112a016.
Cosmidis, J., Benzerara, K., Gheerbrant, E., Estève, I., Bouya, B., Amaghzaz, M., 2013a. Nanometer-scale characterization of exceptionally preserved bacterial fossils in Paleocene phosphorites from Ouled Abdoun (Morocco). Geobiology 11 (2), 139–153. http://dx.doi.org/10.1111/gbi.12022.
Cosmidis, J., Benzerara, K., Menguy, N., Arning, E., 2013b. Microscopy evidence of bacterial microfossils in phosphorite crusts of the Peruvian shelf: Implications for phosphogenesis mechanisms. Chem. Geol. 359, 10–22. http://dx.doi.org/10.1016/j.chemgeo.2013.09.009.
Couradeau, E., Benzerara, K., Gérard, E., Moreira, D., Bernard, S., Brown, G.E., López-García, P., 2012. An early-branching microbialite cyanobacterium forms intracellular carbonates. Science 336 (6080), 459–462. http://dx.doi.org/10.1126/science.1216171.
Cramer, M., Myers, J., 1952. Growth and photosynthetic characteristics of *Euglena gracilis*. Arch. Microbiol. 17 (1), 384–402. http://dx.doi.org/10.1126/science.1216171.
De Gregorio, B.T., Sharp, T.G., 2006. The structure and distribution of carbon in 3.5 Ga Apex chert: Implications for the biogenicity of Earth's oldest putative microfossils. Am. Mineral. 91, 784–789. http://dx.doi.org/10.2138/am.2006.2149.
De Gregorio, B.T., Sharp, T.G., Flynn, G.J., Wirick, S., Hervig, R.L., 2009. Biogenic origin for Earth's oldest putative microfossils. Geology 37 (7), 631–634. http://dx.doi.org/10.1130/G25683A.1.
De Gregorio, B.T., Sharp, T.G., Rushdi, A.I., Simoneit, B.R.T., 2011. Bugs or gunk? Nanoscale methods for assessing the biogenicity of ancient microfossils and organic matter. Earliest Life on Earth: Habitats, Environments and Methods of Detection, pp. 239–289 (ISBN 978-90-481-8793-5).
Dieckmann, V., Schenk, H.J., Horsfield, B., Welte, D.H., 1998. Kinetics of petroleum generation and cracking by programmed-temperature closed-system pyrolysis of Toarcian Shales. Fuel 77 (1), 23–31. http://dx.doi.org/10.1016/S0016-2361(97)00165-8.
Fein, J.B., Scott, S., Rivera, N., 2002. The effect of Fe on Si adsorption by *Bacillus subtilis* cell walls: insights into non-metabolic bacterial precipitation of silicate minerals. Chem. Geol. 182 (2), 265–273. http://dx.doi.org/10.1016/S0009-2541(01)00294-7.
Flörke, O.W., Hollmann, R., Von Rad, U., Rösch, H., 1976. Intergrowth and twinning in opal-CT lepispheres. Contrib. Mineral. Petrol. 58 (3), 235–242. http://dx.doi.org/10.1007/BF00402354.
Fortin, D., Ferris, F.G., 1998. Precipitation of iron, silica, and sulfate on bacterial cell surfaces. Geomicrobiol J. 15 (4), 309–324. http://dx.doi.org/10.1080/01490459809378085.
Foucher, F., Westall, F., 2013. Raman imaging of metastable opal in carbonaceous microfossils of the 700–800 Ma old Draken Formation. Astrobiology 13 (1), 57–67. http://dx.doi.org/10.1089/ast.2012.0889.
Francis, J.T., Hitchcock, A.P., 1992. Inner-shell spectroscopy of *p*-benzoquinone, hydroquinone, and phenol: distinguishing quinoid and benzenoid structures. J. Phys. Chem. 96 (16), 6598–6610. http://dx.doi.org/10.1021/j100195a018.
Francis, S., Barghoorn, E.S., Margulis, L., 1978a. On the experimental silicification of microorganisms. III. Implications of the preservation of the green prokaryotic alga Prochloron and other coccoids for interpretation of the microbial fossil record. Precambrian Res. 7 (4), 377–383. http://dx.doi.org/10.1016/0301-9268(78)90048-7.
Francis, S., Margulis, L., Barghoorn, E.S., 1978b. On the experimental silicification of microorganisms II. On the time of appearance of eukaryotic organisms in the fossil record. Precambrian Res. 6 (1), 65–100. http://dx.doi.org/10.1016/0301-9268(78)90055-4.
Galvez, M.E., Beyssac, O., Benzerara, K., Bernard, S., Menguy, N., Cox, S.C., Brown, G.E., 2012. Morphological preservation of carbonaceous plant fossils in blueschist metamorphic rocks from New Zealand. Geobiology 10 (2), 118–129. http://dx.doi.org/10.1111/j.1472-4669.2011.00316.x.
Gibbs, S.P., 1978. The chloroplasts of Euglena may have evolved from symbiotic green algae. Can. J. Bot. 56 (22), 2883–2889. http://dx.doi.org/10.1139/b78-345.
Glikson, M., Duck, L.J., Golding, S.D., Hofmann, A., Bolhar, R., Webb, R., Baiano, J.C.F., Sly, L.I., 2008. Microbial remains in some earliest Earth rocks: comparison with a potential modern analogue. Precambrian Res. 164 (3), 187–200. http://dx.doi.org/10.1016/j.precamres.2008.05.002.
Grimes, S.T., Brock, F., Rickard, D., Davies, K.L., Edwards, D., Briggs, D.E., Parkes, R.J., 2001. Understanding fossilization: experimental pyritization of plants. Geology 29 (2), 123–126. http://dx.doi.org/10.1130/0091-7613(2001)029<0123:UFEPOP>2.0.CO;2.
Guglielmi, G., Cohen-Bazire, G., Bryant, D.A., 1981. The structure of *Gloeobacter violaceus* and its phycobilisomes. Arch. Microbiol. 129 (3), 181–189. http://dx.doi.org/10.1007/BF01253711.
Guttman, H.N., 1971. Internal cellular details of *Euglena gracilis* visualized by scanning electron microscopy. Science 171 (3968), 290–292. http://dx.doi.org/10.1126/science.171.3968.290.
Handley, K.M., Campbell, K.A., Mountain, B.W., Browne, P.R.L., 2005. Abiotic–biotic controls on the origin and development of spicular sinter: in situ growth experiments. Champagne Pool, Waiotapu, New Zealand. Geobiology 3, 93–114. http://dx.doi.org/10.1111/j.1472-4669.2005.00046.x.
Handley, K.M., Turner, S.J., Campbell, K.A., Mountain, B.W., 2008. Silicifying biofilm exopolymers on a hot-spring microstromatolite: templating nanometer-thick laminae. Astrobiology 8 (4), 747–770. http://dx.doi.org/10.1089/ast.2007.0172.
Hartkopf-Fröder, C., Königshof, P., Littke, R., Schwarzbauer, J., 2015. Optical thermal maturity parameters and organic geochemical alteration at low grade diagenesis to anchimetamorphism: a review. Int. J. Coal Geol. 150, 74–119. http://dx.doi.org/10.1016/j.coal.2015.06.005.
Helgeson, H.C., Knox, A.M., Owens, C.E., Shock, E.L., 1993. Petroleum, oil field waters, and authigenic mineral assemblages: are they in metastable equilibrium in hydrocarbon reservoirs? Geochim. Cosmochim. Acta 57, 3295–3339. http://dx.doi.org/10.1016/0016-7037(93)90541-4.
Helgeson, H.C., Richard, L., McKenzie, W.F., Norton, D.L., Schmitt, A., 2009. A chemical and thermodynamic model of oil generation in hydrocarbon source rocks. Geochim. Cosmochim. Acta 73, 594–695. http://dx.doi.org/10.1016/j.gca.2008.03.004.
Herdianita, N.R., Rodgers, K.A., Browne, P.R., 2000. Routine instrumental procedures to characterise the mineralogy of modern and ancient silica sinters. Geothermics 29 (1), 65–81. http://dx.doi.org/10.1016/S0375-6505(99)00054-1.
Hinman, N.W., 1990. Chemical factors influencing the rates and sequences of silica phase transitions: effects of organic constituents. Geochim. Cosmochim. Acta 54 (6), 1563–1574. http://dx.doi.org/10.1016/0016-7037(90)90391-W.
Hsu, Y.G., Chiang, I.L., Lo, J.F., 2000. Properties of hybrid materials derived from Hydroxy-Containing Linear Polyester and SilicaThrough Sol–Gel Process. I. effect of thermal treatment. J. Appl. Polym. Sci. 78, 1179–1190. http://dx.doi.org/10.1002/1097-4628(20001107)78:6<1179::AID-APP20>3.0.CO;2-T.
Igisu, M., Ueno, Y., Shimojima, M., Nakashima, S., Awramik, S.M., Ohta, H., Maruyama, S., 2009. Micro-FTIR spectroscopic signatures of bacterial lipids in Proterozoic microfossils. Precambrian Res. 173, 19–26. http://dx.doi.org/10.1016/j.precamres.2009.03.006.
Iniesto, M., Zeyen, N., Lopez-Archilla, A.I., Bernard, S., Buscalioni, A.D., Carmen Guerrero, M., Benzerara, K., 2015. Preservation in microbial mats: mineralization by a talc-like phase of a fish embedded in a microbial sarcophagus. Frontiers in Earth Science 3 n °51 http://dx.doi.org/10.3389/feart.2015.00051.
Ishii, I., Hitchcook, A.P., 1988. The oscillator strengths for C1s and O1s excitation of some saturated and unsaturated organic alcohols, acids and esters. J. Electron Spectrosc. Relat. Phenom. 46 (1), 55–84. http://dx.doi.org/10.1016/0368-2048(88)80005-7.
Jal, P.K., Patel, S., Mishra, B.K., 2004. Chemical modification of silica surface by immobilization of functional groups for extractive concentration of metal ions. Talanta 62 (5), 1005–1028. http://dx.doi.org/10.1016/j.talanta.2003.10.028.
Javaux, E.J., Marshall, C.P., Bekker, A., 2010. Organic-walled microfossils in 3.2-billion-year-old shallow-marine siliciclastic deposits. Nature 463 (7283), 934–938. http://dx.doi.org/10.1038/nature08793.
Johansson, L.S., Campbell, J.M., 2004. Reproducible XPS on biopolymers: cellulose studies. Surf. Interface Anal. 36 (8), 1018–1022. http://dx.doi.org/10.1002/sia.1827.
Jones, B., Konhauser, K.O., Renaut, R.W., Wheeler, R.S., 2004. Microbial silicification in Iodine Pool, Waimangu geothermal area, North Island, New Zealand: implications for recognition and identification of ancient silicified microbes. J. Geol. Soc. 161 (6), 983–993. http://dx.doi.org/10.1144/0016-764903-172.
Jones, B., Renaut, R.W., Rosen, M.R., 1998. Microbial biofacies in hot-spring sinters: a model based on Ohaaki Pool, North Island, New Zealand. J. Sediment. Res. 68 (3), 413–434. http://dx.doi.org/10.2110/jsr.68.413.
Jones, B., Renaut, R.W., Rosen, M.R., 2001. Taphonomy of silicified filamentous microbes in modern geothermal sinters—implications for identification. PALAIOS 16 (6), 580–592. http://dx.doi.org/10.1669/0883-1351(2001)016<0580:TOSFMI>2.0.CO;2.
Jones, B., Renaut, R.W., Rosen, M.R., 2003. Silicified microbes in a geyser mound: the enigma of low-temperature cyanobacteria in a high temperature setting. PALAIOS 18, 87–109. http://dx.doi.org/10.1669/0883-1351(2003)18<87:SMIAGM>2.0.CO;2.
Kastner, M., Keene, J.B., Giesekes, J.M., 1977. Diagenesis of siliceous oozes—I. Chemical controls on the rate of opal-A to opal-CT transformation—an experimental study. Geochim. Cosmochim. Acta 41, 1041–1059. http://dx.doi.org/10.1016/0016-7037(77)90099-0.
Konecny, R., 2001. Reactivity of hydroxyl radicals on hydroxylated quartz surface. 1. Cluster model calculations. J. Phys. Chem. B 105 (26), 6221–6226. http://dx.doi.org/10.1021/jp010752v.
Konhauser, K.O., Ferris, F.G., 1996. Diversity of iron and silica precipitation by microbial mats in hydrothermal waters, Iceland: implications for Precambrian iron formations. Geology 24 (4), 323–326. http://dx.doi.org/10.1130/0091-7613(1996)024<0323:DOIASP>2.3.CO;2.
Konhauser, K.O., Jones, B., Phoenix, V.R., Ferris, G., Renaut, R.W., 2004. The microbial role in hot spring silicification. AMBIO: A Journal of the Human Environment 33 (8), 552–558. http://dx.doi.org/10.1579/0044-7447-33.8.552.
Konhauser, K.O., Jones, B., Reysenbach, A.L., Renaut, R.W., 2003. Hot spring sinters: keys to understanding Earth's earliest life forms. Can. J. Earth Sci. 40 (11), 1713–1724. http://dx.doi.org/10.1139/e03-059.
Konhauser, K.O., Phoenix, V.R., Bottrell, S.H., Adams, D.G., Head, I.M., 2001. Microbial–silica interactions in Icelandic hot spring sinter: possible analogues for some Precambrian siliceous stromatolites. Sedimentology 48 (2), 415–433. http://dx.doi.org/10.1046/j.1365-3091.2001.00372.x.
Kremer, B., Kazmierczak, J., Łukomska-Kowalczyk, M., Kempe, S., 2012. Calcification and silicification: fossilization potential of cyanobacteria from stromatolites of Niuafo'ou's Caldera Lakes (Tonga) and implications for the early fossil record. Astrobiology 12 (6), 535–548. http://dx.doi.org/10.1089/ast.2011.0742.
Kyle, J.E., Schroeder, P.A., 2007. Role of smectite in siliceous-sinter formation and microbial-texture preservation: Octopus Spring, Yellowstone National Park, Wyoming, USA. Clay Clay Miner. 55 (2), 189–199. http://dx.doi.org/10.1346/CCMN.2007.0550208.
Lakshtanov, L.Z., Stipp, S.L.S., 2010. Interaction between dissolved silica and calcium carbonate: 1. Spontaneous precipitation of calcium carbonate in the presence of dissolved silica. Geochim. Cosmochim. Acta 74 (9), 2655–2664. http://dx.doi.org/10.1016/j.gca.2010.02.009.
Lalonde, S.V., Konhauser, K.O., Reysenbach, A.L., Ferris, F.G., 2005. The experimental silicification of Aquificales and their role in hot spring sinter formation. Geobiology 3 (1), 41–52. http://dx.doi.org/10.1111/j.1472-4669.2005.00042.x.
Lawrence, J.R., Swerhone, G.D.W., Leppard, G.G., Araki, T., Zhang, X., West, M.M., Hitchcock, A.P., 2003. Scanning transmission X-ray, laser scanning, and transmission electron microscopy mapping of the exopolymeric matrix of microbial biofilms. Appl.

Environ. Microbiol. 69 (9), 5543–5554. http://dx.doi.org/10.1128/AEM.69.9.5543-5554.2003.
Le Guillou, C., Bernard, S., Brearley, A.J., Remusat, L., 2014. Evolution of organic matter in Orgueil, Murchison and Renazzo during parent body aqueous alteration: in situ investigations. Geochim. Cosmochim. Acta 131, 368–392. http://dx.doi.org/10.1016/j.gca.2013.11.020.
Le Guillou, C., Remusat, L., Bernard, S., Brearley, A.J., Leroux, H., 2013. Amorphization and D/H fractionation of kerogens during experimental electron irradiation: comparison with chondritic organic matter. Icarus 226 (1), 101–110. http://dx.doi.org/10.1016/j.icarus.2013.05.003.
Leloup, M., Nicolau, R., Pallier, V., Yéprémian, C., Feuillade-Cathalifaud, G., 2013. Organic matter produced by algae and cyanobacteria: quantitative and qualitative characterization. J. Environ. Sci. 25 (6), 1089–1097. http://dx.doi.org/10.1016/S1001-0742(12)60208-3.
Leo, R.F., Barghoorn, E.S., 1976. Silicification of wood. Bot. Mus. Leafl. Harv. Univ. 25 (1), 1–47.
Lepot, K., Benzerara, K., Brown, G.E., Philippot, P., 2008. Microbially influenced formation of 2,724-million-year-old stromatolites. Nat. Geosci. 1 (2), 118–121. http://dx.doi.org/10.1038/ngeo107.
Lepot, K., Benzerara, K., Rividi, N., Cotte, M., Brown Jr., G.E., Philippot, P., 2009. Organic matter heterogeneities in 2.72 Ga stromatolites: alteration versus preservation by sulfur incorporation. Geochim. Cosmochim. Acta 73, 6579–6599. http://dx.doi.org/10.1016/j.gca.2009.08.014.
Lepot, K., Williford, K.H., Ushikubo, T., Sugitani, K., Mimura, K., Spicuzza, M.J., Valley, J.W., 2013. Texture-specific isotopic compositions in 3.4 Gyr old organic matter support selective preservation in cell-like structures. Geochim. Cosmochim. Acta 112, 66–86. http://dx.doi.org/10.1016/j.gca.2013.03.004.
Lewan, M.D., 1997. Experiments on the role of water in petroleum formation. Geochim. Cosmochim. Acta 61 (17), 3691–3723. http://dx.doi.org/10.1016/S0016-7037(97)00176-2.
Lewan, M.D., Roy, S., 2011. Role of water in hydrocarbon generation from Type-I kerogen in Mahogany oil shale of the Green River Formation. Org. Geochem. 42 (1), 31–41. http://dx.doi.org/10.1016/j.orggeochem.2010.10.004.
Li, J., Benzerara, K., Bernard, S., Beyssac, O., 2013. The link between biomineralization and fossilization of bacteria: insights from field and experimental studies. Chem. Geol. 359, 49–69. http://dx.doi.org/10.1016/j.chemgeo.2013.09.013.
Li, J., Bernard, S., Benzerara, K., Beyssac, O., Allard, T., Cosmidis, J., Moussou, J., 2014. Impact of biomineralization on the preservation of microorganisms during fossilization: an experimental perspective. Earth Planet. Sci. Lett. 400, 113–122. http://dx.doi.org/10.1016/j.epsl.2014.05.031.
Lynne, B.Y., Campbell, K.A., Moore, J.N., Browne, P.R.L., 2005. Diagenesis of 1900-year-old siliceous sinter (opal-A to quartz) at Opal Mound, Roosevelt Hot Springs, Utah, USA. Sediment. Geol. 179 (3), 249–278. http://dx.doi.org/10.1016/j.sedgeo.2005.05.012.
Martin, D., Briggs, D.E., Parkes, R.J., 2003. Experimental mineralization of invertebrate eggs and the preservation of Neoproterozoic embryos. Geology 31 (1), 39–42. http://dx.doi.org/10.1130/0091-7613(2003)031<0039:EMOIEA>2.0.CO;2.
McKenzie, E.J., Brown, K.L., Cady, S.L., Campbell, K.A., 2001. Trace metal chemistry and silicification of microorganisms in geothermal sinter, Taupo Volcanic Zone, New Zealand. Geothermics 30 (4), 483–502. http://dx.doi.org/10.1016/S0375-6505(01)00004-9.
Miot, J., Morin, G., Skouri-Panet, F., Férard, C., Aubry, E., Briand, J., Wang, Y., Ona-Nguema, G., Guyot, F., Brown, G.E., 2008. XAS study of arsenic coordination in *Euglena gracilis* exposed to arsenite. Environ. Sci. Technol. 42 (14), 5342–5347. http://dx.doi.org/10.1021/es703072d.
Miot, J., Morin, G., Skouri-Panet, F., Férard, C., Poitevin, A., Aubry, E., Juillot, F., Ona-Nguema, G., Guyot, F., Brown, G.E., 2009. Speciation of arsenic in *Euglena gracilis* cells exposed to As (V). Environ. Sci. Technol. 43 (9), 3315–3321. http://dx.doi.org/10.1021/es802833s.
Moreau, J.W., Sharp, T.G., 2004. A transmission electron microscopy study of silica and kerogen biosignatures in ~1.9 Ga Gunflint microfossils. Astrobiology 4 (2), 196–210. http://dx.doi.org/10.1089/153110704323175142.
Muscente, A.D., Hawkins, A.D., Xiao, S., 2015. Fossil preservation through phosphatization and silicification in the Ediacaran Doushantuo Formation (South China): a comparative synthesis. Palaeogeogr. Palaeoclimatol. Palaeoecol. 434, 46–62. http://dx.doi.org/10.1016/j.palaeo.2014.10.013.
Nakano, Y., Urade, Y., Urade, R., Kitaoka, S., 1987. Isolation, purification, and characterization of the pellicle of *Euglena gracilis* z. J. Biochem. 102 (5), 1053–1063.
Nassif, N., Bouvet, O., Rager, M.N., Roux, C., Coradin, T., Livage, J., 2002. Living bacteria in silica gels. Nat. Mater. 1 (1), 42–44. http://dx.doi.org/10.1038/nmat709.
Oehler, J.H., 1976a. Experimental studies in Precambrian paleontology: structural and chemical changes in blue-green algae during simulated fossilization in synthetic chert. Geol. Soc. Am. Bull. 87 (1), 117–129. http://dx.doi.org/10.1130/0016-7606(1976)87<117:ESIPPS>2.0.CO;2.
Oehler, J.H., 1976b. Hydrothermal crystallization of silica gel. Geol. Soc. Am. Bull. 87 (8), 1143–1152. http://dx.doi.org/10.1130/0016-7606(1976)87<1143:HCOSG>2.0.CO;2.
Oehler, J.H., Schopf, J.W., 1971. Artificial microfossils: experimental studies of permineralization of blue-green algae in silica. Science 174 (4015), 1229–1231. http://dx.doi.org/10.1126/science.174.4015.1229.
Okamoto, A., Saishu, H., Hirano, N., Tsuchiya, N., 2010. Mineralogical and textural variation of silica minerals in hydrothermal flow-through experiments: Implications for quartz vein formation. Geochim. Cosmochim. Acta 74 (13), 3692–3706. http://dx.doi.org/10.1016/j.gca.2010.03.031.
Orange, F., Chabin, A., Gorlas, A., Lucas-Staat, S., Geslin, C., Le Romancer, M., Prangishvili, D., Forterre, P., Westall, F., 2011a. Experimental fossilisation of viruses from extremophilic Archaea. Biogeosciences 8 (6), 1465–1475. http://dx.doi.org/10.5194/bg-8-1465-2011.
Orange, F., Disnar, J.R., Gautret, P., Westall, F., Bienvenu, N., Lottier, N., Prieur, D., 2012. Preservation and evolution of organic matter during experimental fossilisation of the hyperthermophilic archaea Methanocaldococcus jannaschii. Orig. Life Evol. Biosph. 42 (6), 587–609. http://dx.doi.org/10.1007/s11084-012-9318-x.
Orange, F., Disnar, J.R., Westall, F., Prieur, D., Baillif, P., 2011b. Metal cation binding by the hyperthermophilic microorganism, Archaea *Methanocaldococcus jannaschii*, and its effects on silicification. Palaeontology 54 (5), 953–964. http://dx.doi.org/10.1111/j.1475-4983.2011.01066.x.
Orange, F., Dupont, S., Goff, O.L., Bienvenu, N., Disnar, J.R., Westall, F., Le Romancer, M., 2014. Experimental fossilization of the thermophilic Gram-positive Bacterium Geobacillus SP7A: a long duration preservation study. Geomicrobiol J. 31 (7), 578–589. http://dx.doi.org/10.1080/01490451.2013.860208.
Orange, F., Lalonde, S.V., Konhauser, K.O., 2013a. Experimental simulation of evaporation-driven silica sinter formation and microbial silicification in hot spring systems. Astrobiology 13 (2), 163–176. http://dx.doi.org/10.1089/ast.2012.0887.
Orange, F., Lalonde, S.V., Konhauser, K.O., 2013b. The formation and preservation of *Synechococcus elongatus* cell molds in simulated silica sinter: implications for the identification of microfossils. Geomicrobiol J. 30 (4), 327–336. http://dx.doi.org/10.1080/01490451.2012.688926.
Orange, F., Westall, F., Disnar, J.R., Prieur, D., Bienvenu, N., Le Romancer, M., Défarge, C., 2009. Experimental silicification of the extremophilic Archaea Pyrococcus abyssi and Methanocaldococcus jannaschii: applications in the search for evidence of life in early Earth and extraterrestrial rocks. Geobiology 7 (4), 403–418. http://dx.doi.org/10.1111/j.1472-4669.2009.00212.x.
Orr, P.J., Briggs, D.E.G., Kearns, S.L., 1998. Cambrian Burgess Shale animals replicated in clay minerals. Science 281, 1173–1175. http://dx.doi.org/10.1126/science.281.5380.1173.
Pérez-Maqueda, L.A., Sánchez-Jiménez, P.E., Perejón, A., García-Garrido, C., Criado, J.M., Benítez-Guerrero, M., 2014. Scission kinetic model for the prediction of polymer pyrolysis curves from chain structure. Polym. Test. 37, 1–5. http://dx.doi.org/10.1016/j.polymertesting.2014.04.004.
Phoenix, V.R., Adams, D.G., Konhauser, K.O., 2000. Cyanobacterial viability during hydrothermal biomineralisation. Chem. Geol. 169, 329–338. http://dx.doi.org/10.1016/S0009-2541(00)00212-6.
Picard, A., Kappler, A., Schmid, G., Quaroni, L., Obst, M., 2015a. Experimental diagenesis of organo-mineral structures formed by microaerophilic Fe (II)-oxidizing bacteria. Nat. Commun. 6. http://dx.doi.org/10.1038/ncomms7277.
Picard, A., Obst, M., Schmid, G., Zeitvogel, F., Kappler, A., 2015b. Limited influence of Si on the preservation of Fe mineral-encrusted microbial cells during experimental diagenesis. Geobiology http://dx.doi.org/10.1111/gbi.12171.
Ravel, B., Newville, M., 2005. ATHENA, ARTEMIS, HEPHAESTUS: data analysis for X-ray absorption spectroscopy using IFEFFIT. J. Synchrotron Radiat. 12 (4), 537–541. http://dx.doi.org/10.1107/S0909049505012719.
Regier, T., Krochak, J., Sham, T.K., Hu, Y.F., Thompson, J., Blyth, R.I.R., 2007. Performance and capabilities of the Canadian Dragon: the SGM beamline at the Canadian Light Source. Nucl. Inst. Methods Phys. Res. A 582 (1), 93–95. http://dx.doi.org/10.1016/j.nima.2007.08.071.
Rexroth, S., Mullineaux, C.W., Ellinger, D., Sendtko, E., Rögner, M., Koenig, F., 2011. The plasma membrane of the cyanobacterium Gloeobacter violaceus contains segregated bioenergetic domains. Plant Cell 23 (6), 2379–2390. http://dx.doi.org/10.1105/tpc.111.085779.
Richard, L., Helgeson, H.C., 1998. Calculation of the thermodynamic properties at elevated temperatures and pressures of saturated and aromatic high molecular weight solid and liquid hydrocarbons in kerogen, bitumen, petroleum, and other organic matter of biogeochemical interest. Geochim. Cosmochim. Acta 62, 3591–3636. http://dx.doi.org/10.1016/S0016-7037(97)00345-1.
Rimstidt, J.D., Cole, D.R., 1983. Geothermal mineralization; I, the mechanism of formation of the Beowawe, Nevada, siliceous sinter deposit. Am. J. Sci. 283 (8), 861–875. http://dx.doi.org/10.2475/ajs.283.8.861.
Rippka, R., Waterbury, J., Cohen-Bazire, G., 1974. A cyanobacterium which lacks thylakoids. Arch. Microbiol. 100 (1), 419–436. http://dx.doi.org/10.1007/BF00446333.
Robin, N., Bernard, S., Miot, J., Blanc-Valleron, M.-M., Charbonnier, S., Petit, G., 2015. Calcification and diagenesis of bacterial colonies. Minerals 5, 488–506. http://dx.doi.org/10.3390/min5030488.
Rodgers, K.A., Browne, P.R.L., Buddle, T.F., Cook, K.L., Greatrex, R.A., Hampton, W.A., Herdianita, N.R., Holland, G.R., Lynne, B.Y., Martin, R., Newton, Z., Pastars, D., Sannazarro, K.L., Teece, C.I.A., 2004. Silica phases in sinters and residues from geothermal fields of New Zealand. Earth Sci. Rev. 66 (1), 1–61. http://dx.doi.org/10.1016/j.earscirev.2003.10.001.
Rothenberg, G., Downie, A.P., Raston, C.L., Scott, J.L., 2001. Understanding solid/solid organic reactions. J. Am. Chem. Soc. 123 (36), 8701–8708. http://dx.doi.org/10.1021/ja0034388.
Rouchon, V., Bernard, S., 2015. Mapping iron gall ink penetration within paper fibres using scanning transmission X-ray microscopy. J. Anal. At. Spectrom. 30 (3), 635–641. http://dx.doi.org/10.1039/C4JA00358F.
Sánchez-Jiménez, P.E., Pérez-Maqueda, L.A., Perejón, A., Criado, J.M., 2010. Generalized kinetic master plots for the thermal degradation of polymers following a random scission mechanism. The Journal of Physical Chemistry A 114 (30), 7868–7876. http://dx.doi.org/10.1021/jp103171h.
Schiffbauer, J.D., Wallace, A.F., Hunter, J.L., Kowalewski, M., Bodnar, R.J., Xiao, S., 2012. Thermally-induced structural and chemical alteration of organic-walled microfossils: an experimental approach to understanding fossil preservation in metasediments. Geobiology 10 (5), 402–423. http://dx.doi.org/10.1111/j.1472-4669.2012.00332.x.
Schiffbauer, J.D., Xiao, S., Cai, Y., Wallace, A.F., Hua, H., Hunter, J., Xu, H., Peng, Y., Kaufman, A.J., 2014. A unifying model for Neoproterozoic–Palaeozoic exceptional fossil preservation through pyritization and carbonaceous compression. Nat. Commun. 5. http://dx.doi.org/10.1038/ncomms6754.

Schneider, S., Jürgens, U.J., 1991. Cell wall and sheath constituents of the cyanobacterium Gloeobacter violaceus. Arch. Microbiol. 156 (4), 312–318. http://dx.doi.org/10.1007/BF00263004.
Schopf, J.W., Kudryavtsev, A.B., 2012. Biogenicity of Earth's earliest fossils: a resolution of the controversy. Gondwana Res. 22 (3), 761–771. http://dx.doi.org/10.1016/j.gr.2012.07.003.
Schopf, J.W., Kudryavtsev, A.B., Agresti, D.G., Wdowiak, T.J., Czaja, A.D., 2002. Laser–Raman imagery of Earth's earliest fossils. Nature 416 (6876), 73–76. http://dx.doi.org/10.1038/416073a.
Schultze-Lam, S., Ferris, F.G., Konhauser, K.O., Wiese, R.G., 1995. *In situ* silicification of an Icelandic hot spring microbial mat: implications for microfossil formation. Can. J. Earth Sci. 32 (12), 2021–2026. http://dx.doi.org/10.1139/e95-155.
Solomon, D., Lehmann, J., Kinyangi, J., Liang, B., Heymann, K., Dathe, L., Hanley, K., Wirick, S., Jacobsen, C., 2009. Carbon (1s) NEXAFS spectroscopy of biogeochemically relevant reference organic compounds. Soil Sci. Soc. Am. J. 73 (6), 1817–1830. http://dx.doi.org/10.2136/sssaj2008.0228.
Sommer, J.R., 1965. The ultrastructure of the pellicle complex of *Euglena gracilis*. J. Cell Biol. 24 (2), 253–257. http://dx.doi.org/10.1083/jcb.24.2.253.
Sugitani, K., Mimura, K., Takeuchi, M., Lepot, K., Ito, S., Javaux, E.J., 2015a. Early evolution of large micro-organisms with cytological complexity revealed by microanalyses of 3.4 Ga organic-walled microfossils. Geobiology 13 (6), 507–521. http://dx.doi.org/10.1111/gbi.12148.
Sugitani, K., Mimura, K., Takeuchi, M., Yamaguchi, T., Suzuki, K., Senda, R., Asahara, Y., Wallis, S., Van Kranendonk, M.J., 2015b. A Paleoarchean coastal hydrothermal field inhabited by diverse microbial communities: the Strelley Pool Formation, Pilbara Craton, Western Australia. Geobiology 13 (6), 522–545. http://dx.doi.org/10.1111/gbi.12150.
Sugitani, K., Grey, K., Allwood, A., Nagaoka, T., Mimura, K., Minami, M., Marshall, C.P., Van Kranendonk, M.J., Walter, M.R., 2007. Diverse microstructures from Archaean chert from the Mount Goldsworthy–Mount Grant area, Pilbara Craton, Western Australia: microfossils, dubiofossils, or pseudofossils? Precambrian Res. 158, 228–262. http://dx.doi.org/10.1016/j.precamres.2007.03.006.
Sugitani, K., Lepot, K., Nagaoka, T., Mimura, K., Van Kranendonk, M., Oehler, D.Z., Walter, M.R., 2010. Biogenicity of morphologically diverse carbonaceous microstructures from the ca. 3400 Ma Strelley Pool Formation, in the Pilbara Craton, Western Australia. Astrobiology 10 (9), 899–920. http://dx.doi.org/10.1089/ast.2010.0513.
Sugitani, K., Mimura, K., Nagaoka, T., Lepot, K., Takeuchi, M., 2013. Microfossil assemblage from the 3400 Ma Strelley Pool Formation in the Pilbara Craton, Western Australia: Results form a new locality. Precambrian Res. 226, 59–74. http://dx.doi.org/10.1016/j.precamres.2012.11.005.
Tice, M.M., Lowe, D.R., 2004. Photosynthetic microbial mats in the 3,416-Myr-old ocean. Nature 431 (7008), 549–552. http://dx.doi.org/10.1038/nature02888.
Tice, M.M., Lowe, D.R., 2006. The origin of carbonaceous matter in pre-3.0 Ga greenstone terrains: a review and new evidence from the 3.42 Ga Buck Reef Chert. Earth Sci. Rev. 76 (3), 259–300. http://dx.doi.org/10.1016/j.earscirev.2006.03.003.
Tice, M.M., Bostick, B.C., Lowe, D.R., 2004. Thermal history of the 3.5–3.2 Ga Onverwacht and Fig Tree Groups, Barberton greenstone belt, South Africa, inferred by Raman microspectroscopy of carbonaceous material. Geology 32 (1), 37–40. http://dx.doi.org/10.1130/G19915.1.
Toporski, J.K., Steele, A., Westall, F., Thomas-Keprta, K.L., McKay, D.S., 2002. The simulated silicification of bacteria-new clues to the modes and timing of bacterial preservation and implications for the search for extraterrestrial microfossils. Astrobiology 2 (1), 1–26. http://dx.doi.org/10.1089/153110702753621312.
Ueno, Y., Isozaki, Y., McNamara, K.J., 2006. Coccoid-like microstructures in a 3.0 Ga chert from Western Australia. Int. Geol. Rev. 48 (1), 78–88. http://dx.doi.org/10.2747/0020-6814.48.1.78.
Ueno, Y., Isozaki, Y., Yurimoto, H., Maruyama, S., 2001. Carbon isotopic signatures of individual Archean microfossils (?) from Western Australia. Int. Geol. Rev. 43 (3), 196–212. http://dx.doi.org/10.1080/00206810109465008.
Vandenbroucke, M., Largeau, C., 2007. Kerogen origin, evolution and structure. Org. Geochem. 38 (5), 719–833. http://dx.doi.org/10.1016/j.orggeochem.2007.01.001.
Vismara, R., Barsanti, L., Lupetti, P., Passarelli, V., Mercati, D., Dallai, R., Gualtieri, P., 2000. Ultrastructure of the pellicle of *Euglena gracilis*. Tissue Cell 32 (6), 451–456. http://dx.doi.org/10.1016/S0040-8166(00)80001-4.
Wacey, D., Kilburn, M.R., Saunders, M., Cliff, J., Brasier, M.D., 2011a. Microfossils of sulphur-metabolizing cells in 3.4-billion-year-old rocks of Western Australia. Nat. Geosci. 4 (10), 698–702. http://dx.doi.org/10.1038/NGEO1238.
Wacey, D., Menon, S., Green, L., Gerstmann, D., Kong, C., Mcloughlin, N., Saunders, M., Brasier, M., 2012. Taphonomy of very ancient microfossils from the ~3400 Ma Strelley Pool Formation and ~1900Ma Gunflint Formation: new insights using a focused ion beam. Precambrian Res. 220, 234–250. http://dx.doi.org/10.1016/j.precamres.2012.08.005.
Wacey, D., Saunders, M., Brasier, M.D., Kilburn, M.R., 2011b. Earliest microbially mediated pyrite oxidation in ~3.4 billion-year-old sediments. Earth Planet. Sci. Lett. 301 (1), 393–402. http://dx.doi.org/10.1016/j.epsl.2010.11.025.
Wacey, D., Saunders, M., Kong, C., Brasier, A., Brasier, M.D., 2015. 3.46 Ga Apex chert 'microfossils' reinterpreted as mineral artefacts produced during phyllosilicate exfoliation. Gondwana Res. http://dx.doi.org/10.1016/j.gr.2015.07.010.
Wacey, D., Saunders, M., Roberts, M., Menon, S., Green, L., Kong, C., Culwick, T., Strother, P., Brasier, M.D., 2014. Enhanced cellular preservation by clay minerals in 1 billion-year-old lakes. Sci. Report. 4. http://dx.doi.org/10.1038/srep05841.
Walsh, M.M., Lowe, D.R., 1985. Filamentous microfossils from the 3,500-Myr-old Onverwacht Group, Barberton Mountain Land, South Africa. Nature 314, 530–532. http://dx.doi.org/10.1038/314530a0.
Walter, M.R., Bauld, J., Brock, T.D., 1972. Siliceous algal and bacterial stromatolites in hot spring and geyser effluents of Yellowstone National Park. Science 178 (4059), 402–405. http://dx.doi.org/10.1126/science.178.4059.402.
Walters, C.C., Margulis, L., Barghoorn, E.S., 1977. On the experimental silicification of microorganisms, I. Microbial growth on organosilicon compounds. Precambrian Res. 5 (3), 241–248. http://dx.doi.org/10.1016/0301-9268(77)90031-6.
Westall, F., Boni, L., Guerzoni, E., 1995. The experimental silicification of microorganisms. Palaeontology 38 (3), 495–528.
Westall, F., Campbell, K.A., Bréhéret, J.G., Foucher, F., Gautret, P., Hubert, A., Sorieul, S., Grassineau, N., Guido, D.M., 2015. Archean (3.33 Ga) microbe-sediment systems were diverse and flourished in a hydrothermal context. Geology 43 (7), 615–618. http://dx.doi.org/10.1130/G36646.1.
Westall, F., De Ronde, C.E., Southam, G., Grassineau, N., Colas, M., Cockell, C., Lammer, H., 2006. Implications of a 3.472–3.333 Gyr-old subaerial microbial mat from the Barberton greenstone belt, South Africa for the UV environmental conditions on the early Earth. Philosophical Transactions of the Royal Society of London B: Biological Sciences 361 (1474), 1857–1876. http://dx.doi.org/10.1098/rstb.2006.1896.
Westall, F., de Wit, M.J., Dann, J., van der Gaast, S., de Ronde, C.E., Gerneke, D., 2001. Early Archean fossil bacteria and biofilms in hydrothermally-influenced sediments from the Barberton greenstone belt, South Africa. Precambrian Res. 106 (1), 93–116. http://dx.doi.org/10.1016/S0301-9268(00)00127-3.
Westall, F., Foucher, F., Cavalazzi, B., De Vries, S.T., Nijman, W., Pearson, V., Watson, J., Verchovsky, A., Wright, I., Rouzaud, J.-N., Marchesini, D., Anne, S., 2011. Volcaniclastic habitats for early life on Earth and Mars: a case study from ~3.5 Ga-old rocks from the Pilbara, Australia. Planetary and Space Science 59 (10), 1093–1106. http://dx.doi.org/10.1016/j.pss.2010.09.006.
Williams, D.L., 2016. Light and the evolution of vision. Eye 1–6 http://dx.doi.org/10.1038/eye.2015.220.
Wilson, L.A., Butterfield, N.J., 2014. Sediment effects on the preservation of Burgess Shale-type compression fossils. PALAIOS 29 (4), 145–154. http://dx.doi.org/10.2110/palo.2013.075.
Xiao, S., Schiffbauer, J.D., 2009. Microfossil phosphatization and its astrobiological implications. In: Seckbach, J., Walsh, M. (Eds.), From Fossils to Astrobiology. Springer Science, Berlin, Germany, pp. 89–117.
Yee, N., Phoenix, V.R., Konhauser, K.O., Benning, L.G., Ferris, F.G., 2003. The effect of cyanobacteria on silica precipitation at neutral pH: implications for bacterial silicification in geothermal hot springs. Chem. Geol. 199 (1), 83–90. http://dx.doi.org/10.1016/S0009-2541(03)00120-7.
Zhao, Y., Wei, F., Yu, Y., 2010. Effects of reaction time and temperature on carbonization in asphaltene pyrolysis. J. Pet. Sci. Eng. 74 (1), 20–25. http://dx.doi.org/10.1016/j.petrol.2010.08.002.
Zhuravlev, L.T., 2000. The surface chemistry of amorphous silica. Zhuravlev model. Colloids Surf. A Physicochem. Eng. Asp. 173 (1), 1–38. http://dx.doi.org/10.1016/S0927-7757(00)00556-2.
Zou, H., Hu, S., Shen, J., 2008. Polymer/silica nanocomposites: preparation, characterization, properties, and applications. Chem. Rev. 108, 3893–3957. http://dx.doi.org/10.1021/cr068035q.